Induction of α-Helix in the β-Sheet Protein Tumor Necrosis Factor-α: Thermal- and Trifluoroethanol-Induced Denaturation at Neutral pH

Linda Owers Narhi,* John S. Philo, Tiansheng Li, Mei Zhang, Babru Samal, and Tsutomu Arakawa

Amgen Inc., Amgen Center, M/S 14-2-D, Thousand Oaks, California 91320-1789

Received November 21, 1995; Revised Manuscript Received March 27, 1996[⊗]

ABSTRACT: The unfolding and refolding of α-helical proteins has been extensively studied, demonstrating formation of intermediate structures which retain the native-like α-helix but lack the tertiary structure. Studies on the folding of proteins consisting primarily of β-sheet are interesting since, unlike the α-helix, the β-sheet requires the formation of peptide hydrogen bonds between two or more polypeptide segments which may be far apart in the linear sequence. Here we have studied the unfolding of the β-sheet-containing protein tumor necrosis factor-α (TNF-α). This protein exists as a symmetric trimer in solution. Murine TNF-α begins to melt at 60 °C and unfolds to a soluble structure with a transition midpoint of 66 °C. This reaction is irreversible. This unfolded form contains a considerable amount of (∼30%) α-helix, as determined by circular dichroism. Human TNF-α begins to melt at 60 °C and precipitates concurrently with unfolding, such that there is no soluble protein present by 70 °C. The secondary and tertiary structures of murine TNF-α unfold simultaneously, suggesting that unfolding from the native to the unfolded state occurs cooperatively. The thermal-induced denaturation is very insensitive to protein concentration, indicating that trimer to monomer conversion, if it occurs, is not rate-limiting. Trifluoroethanol induces α-helix in both human and murine TNF-α, further demonstrating the propensity of TNF-α to form α-helix. The different behavior of human versus murine TNF-α upon thermal unfolding is due to differences in the solubility of the unfolded protein, the murine form being more soluble. These results indicate that TNF-α can form α-helix when the long range interactions conferred by the native structure are removed during unfolding.

Tumor necrosis factor-α (TNF-α),[1] first observed by Carswell et al. (1975), plays an important role as a mediator of inflammation and the immune response (Ming et al., 1987; Sherry & Cerami, 1988). Human TNF-α, synthesized initially as a precursor form of 233 amino acids, is post-translationally processed to the mature form containing the 155 C-terminal amino acids (Yamada et al., 1985). Full activity is obtained with the C-terminal 148 amino acids (Yamagashi et al., 1989). TNF-α is a β-sheet protein which self-associates into a symmetrical trimer (Arakawa & Yphantis, 1987; Davis et al., 1987; Narhi et al., 1987; Lewitt-Bentley et al., 1988; Eck & Sprang, 1989; Jones et al., 1989).

The unfolding and refolding of proteins, in particular of α-helical proteins, has been extensively studied, resulting in the well-characterized "framework model" (Kuwajima, 1989; Kim & Baldwin, 1990). In this model, the unfolded protein first forms core α-helical structures and these helices fold into a compact tertiary structure. The unfolding and refolding of proteins which contain only β-sheet, such as TNF-α, have been less extensively studied. Shiraki and colleagues have recently demonstrated the formation of α-helix during the TFE-induced unfolding of many different proteins, including the β-sheet protein β-lactoglobin (Shiraki et al., 1995). Studies on the unfolding of other proteins containing substantial β-sheet, such as cardiotoxin analogue III (Kumar et al., 1995), ubiquitin (Wilkinson & Mayer, 1986; Briggs & Roder, 1992), interleukin-1β (Clare et al., 1991; Varley et al., 1993), and rat fatty acid binding protein (Ropson et al., 1990; Ropson & Frieden, 1992), identified intermediate forms which contained β-sheet structure as predicted. In this paper, we have examined the unfolding of murine and human TNF-α induced by either high temperatures or TFE. TFE-induced unfolding of both proteins, and thermal-induced denaturation of murine TNF-α, resulted in induction of α-helical conformation. The thermal-induced unfolding of human TNF-α resulted in precipitation, due to the difference in hydrophobicity between human and murine TNF-α. The unfolded form of murine TNF-α at neutral pH, induced by either heat or TFE, contains α-helical structures when analyzed by CD and FTIR. This secondary structure is not present in the folded protein. In this paper, we report the characterization of the structure of TNF-α at neutral pH in these non-native environments.

MATERIALS AND METHODS

TNF-α Preparation. Recombinant human TNF-α was purified from *Escherichia coli* as described previously (Davis et al., 1987). The recombinant murine TNF-α was purified using the same procedure. Protein concentrations were determined from the absorbance at 280 nm, assuming an $\epsilon_{280}^{0.1\%}$ of 1.26 for the murine molecule and 1.19 for the human molecule. All analyses were performed in Dulbecco's PBS unless otherwise noted.

* To whom correspondence should be addressed at. Phone: 805-447-3104. Fax: 805-499-7464.

[⊗] Abstract published in *Advance ACS Abstracts,* August 15, 1996.

[1] Abbreviations: TNF-α, tumor necrosis factor-α; FTIR, Fourier transform infrared; SEC, size exclusion chromatography; PBS, phosphate-buffered saline; HPLC, high-performance liquid chromatography; TFE, trifluoroethanol; ANS, 1,8-anilinonaphthalene sulfonate.

S0006-2960(95)02766-8 CCC: $12.00

Circular Dichroism. The CD spectra were determined on a Jasco J-720 spectropolarimeter controlled by a DOS-based computer and Jasco software using cylindrical cuvettes with a path length of 0.02 cm for the far-UV region (250−190 nm) and a path length of 1 cm for the near-UV region (340−240 nm). Spectra represent the average of 10 accumulations collected at 10 and 20 nm/min, respectively, at a resolution of 0.1 nm. Thermal denaturation was performed on the same instrument using a Peltier thermal control JTC-343 unit, a heating rate of 20 °C/h, and a rectangular cuvette with a path length of 0.1 cm. Mean residue ellipticity was calculated assuming a mean residue weight of 111.2. The TFE titration was performed on a Jasco J-500C spectropolarimeter, by mixing H_2O and TFE with 40 μL of the TNF-α to obtain the desired percentage of TFE. The amount of α-helix was determined from the ellipticity at 208 nm using the Greenfield−Fasman equation (Greenfield & Fasman, 1969). The spectra could not be accurately fit by deconvolution.

ANS Titration. ANS titration (obtained from Molecular Probes and added as a 1 mM stock in water) was done using protein solutions of 0.25 mg/mL, exciting the solution at 380 nm, and following the change in fluorescence between 400 and 550 nm upon ANS addition (25−250 μM ANS). Fluorescence spectra were determined on an SLM-Aminco SPF-500 spectrofluorimeter using a 0.5 cm cuvette.

Infrared Spectroscopy. Solutions of the TNF-α samples were prepared for IR spectroscopy by exchanging solutions in H_2O into a PBS buffer prepared in D_2O using Centricon-10 microconcentrators (Amicon) and concentrating the proteins to ∼30 mg/mL. IR spectra from 1760 to 1600 wavenumbers were measured with a Mattson research series FTIR spectrometer (ATI Instruments, Madison, WI) using a liquid nitrogen-cooled MCT detector. For each spectrum, 4000 scans were coadded at a resolution of 2 cm^{-1}. Spectra were analyzed according to Susi and Byler (1983) as described by Prestrelski et al. (1991).

Sedimentation Equilibrium. Sedimentation equilibrium experiments were carried out at 25 °C using six-channel charcoal-Epon cells in a Beckman XL-A analytical ultracentrifuge. Murine TNF-α was loaded at 0.44 mg/mL and 2-, 4-, 16-, and 32-fold dilutions and run at 10 000, 14 000, and 20 000 rpm. Human TNF-α was loaded at 0.4 mg/mL and 8-, 15-, and 32-fold dilutions (two samples at each concentration), plus a single sample at 0.2 mg/mL, and run at 10 000 and 14 000 rpm. Concentration distributions were measured at 280 or 230 nm. Samples were equilibrated at each speed for at least 24 h, and attainment of equilibrium was verified by the constancy of scans taken 4 h apart. At the conclusion of a run, the rotor was taken to 48 000 rpm for 18 h to force all the protein to the bottom of the cell. Scans of the upper portions of each channel at this high speed were used to establish a baseline absorbance level for each sample, and this baseline offset was subtracted from the data before further processing. A density of 1.003 99 g/mL for the PBS buffer was determined with a Paar density meter. Partial specific volumes of 0.7416 and 0.7401 mL/g for murine and human TNF-α, respectively, were calculated from their amino acid composition (Laue et al., 1992).

Simultaneous analysis of data from multiple samples and speeds was carried out using nonlinear least squares techniques similar to those in NONLIN (Johnson et al., 1981), using the program KDALTON developed in-house. Confidence intervals for the parameters were evaluated using the "preferred method" outlined by Johnson and Faunt (1992).

Sedimentation Velocity. The experimental procedures and methods of analysis are described in the following paper (Narhi et al., 1996).

HPLC. Analysis of the dissociation of murine and human TNF-α by SEC−HPLC was performed as described previously (Narhi & Arakawa, 1987). Briefly, HPLC was performed with a Beckman System gold and a WISP autosampler; 120 μL samples of protein were injected onto a BioRad TSK 250 Bio-Sil column (7.5 × 60 cm) and eluted with a flow rate of 1 mL/min, while monitoring the absorbance at 214 nm. The Maxima Chromatography Station was used to collect and analyze the data.

RESULTS

Thermal Unfolding. The thermal unfolding of murine and human TNF-α was studied by following changes in the far-UV CD spectra as the proteins were heated. Figure 1A shows the heat-induced change in spectra of murine TNF-α, while Figure 1B shows the plot of ellipticity (θ) at 215 nm versus temperature obtained for both proteins. This wavelength was used as it is the minimum for the native protein, and the noise does not increase with temperature at this wavelength. The murine TNF-α melts with a cooperative transition between 60 and 70 °C. The apparent transition midpoint occurs at 66 °C as shown by an arrow in panel B. Since this unfolding is irreversible, this is not a thermodynamic parameter. The intensity of the negative ellipticity from 200 to 220 nm increases greatly as the molecule unfolds, to about −12 000 at 208 nm, indicating substantial formation of α-helix (∼30%). The formation of α-helix makes it difficult to see if the β-sheet structure remains after thermal unfolding, as helix has a much stronger signal in this region. The spectrum of the human molecule, in contrast, begins changing at 60 °C from a β-sheet spectrum to that of the blank. This is accompanied by the formation of visible precipitates. There is no protein left in solution by 70 °C. These results indicate that the unfolded form of the human molecule has a much greater propensity to aggregate and precipitate than that of the murine TNF-α, while the stability of the folded form of both proteins is very similar.

The near-UV CD signal throughout the spectra from 340 to 240 nm approached zero upon heating as shown in Figure 2, indicating that all tertiary structure is lost, and this occurs at the same temperature as the changes in the secondary structure. Therefore, the loss of tertiary structure is accompanied by induction of α-helix. This could indicate that long range interactions conferred by the native structure favor β-sheet conformation and the protein has a propensity to form α-helices in the absence of these interactions. This is consistent with secondary structure prediction based on the sequence, which indicates clusters of amino acids with α-helical propensity (Figure 3), and is in agreement with Shiraki and co-workers (1995) and work from other labs indicating that the structure adopted by proteins following unfolding more closely resembles the structure of peptides derived from the proteins (Dyson et al., 1992a,b; Kemmink & Creighton, 1993; Kwon & Kim, 1994) or the reduced protein than that of the folded protein.

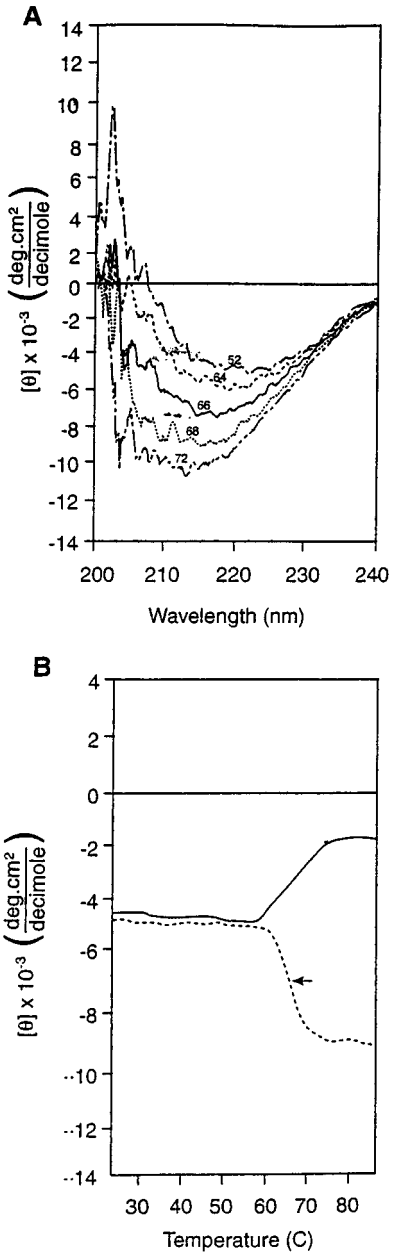

FIGURE 1: Temperature dependence of far-UV CD. (A) Plot of the far-UV CD spectra of murine TNF-α over the transition region obtained during thermal denaturation. The numbers indicate the temperature at which the spectrum was acquired. (B) Thermal stability of human (—) and murine (- - -) TNF-α, as determined by monitoring the CD signal at 215 nm as a function of increasing temperature; the arrow indicates the midpoint of the murine TNF-α transition.

The effect of protein concentration on the thermal denaturation of murine TNF-α was determined and is shown in Figure 2. The unfolding remains irreversible even at the lowest protein concentrations. Since this is an irreversible reaction, the unfolding experiments may reflect kinetics rather than thermodynamics. The thermal-induced denaturation is very insensitive to protein concentration, with melting occurring at the same temperature regardless of whether the protein is at 1 or 0.01 mg/mL. This indicates that a change in conformation of the protein, rather than a change in oligomeric state (if in fact this occurs), must be the rate-limiting step.

The structure of unfolded TNF-α was more fully examined. The murine TNF-α was heated to 65 °C and the CD spectrum taken at this temperature with a much slower

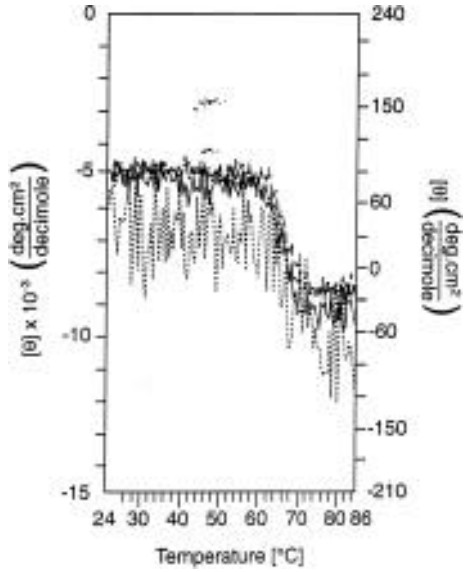

FIGURE 2: Effect of protein concentration on the thermal stability of murine TNF-α in PBS, as determined by monitoring the CD signal as a function of increasing temperature. The change in the ellipticity of near-UV CD spectra at 280 nm and 0.48 mg/mL is shown (••—••) with the scale on the right. The change in the ellipticity of the far-UV CD spectra at 215 nm at 0.4 mg/mL (—), 1 mg/mL (- - -), and 0.01 mg/mL (—•—) is also shown. The scale for the far-UV experiments is on the left.

wavelength scan rate. It was identical to the spectra obtained at elevated temperatures during melting, only with less noise, and was consistent with α-helix induction. A CD spectrum identical to that at 65 °C was observed upon cooling, indicating that unfolding of the murine TNF-α is irreversible and the α-helix structure persists after cooling. The cooled sample showed aggregates of widely ranging sizes when analyzed by sedimentation velocity (data not shown).

A small amount of denaturant is often included during heating of proteins to increase the reversibility of the reaction when unfolding is irreversible due to aggregation. When murine TNF-α was heated in the presence of 2 M urea the same amount of α-helix was induced, at a decreased melting temperature. However, there was no change in the reversibility of unfolding. This result combined with the irreversibility of melting at 0.01 mg/mL and the insensitivity of the reaction to protein concentration could indicate that the α-helical conformation, once obtained, is very stable itself and then aggregates under appropriate conditions. Alternatively, once the α-helical structure is achieved, the aggregate could form more quickly than the native structure, allowing for kinetic control of this pathway. Similar results are obtained for the folding/aggregation of p22 tailspike protein (King, 1989; Mitrake et al., 1991).

TFE-Induced Unfolding. The effect of TFE on the spectra of both human and murine TNF-α was also assessed; the far-UV CD spectra obtained in 60% TFE are shown in Figure 4, while the inset shows the change in ellipticity of murine TNF-α with TFE concentration. The human TNF-α precipitates slightly at 10 and 20% TFE but is then soluble again at 40 and 60% TFE. This is consistent with the decreased solubility of the human TNF-α relative to the murine following heat-induced denaturation.

Substantial (20−40%) α-helix is induced in both proteins accompanied by the loss of β-sheet. This is consistent with the amount of helix formed during thermal-induced denaturation and is further evidence that the amino acid sequence

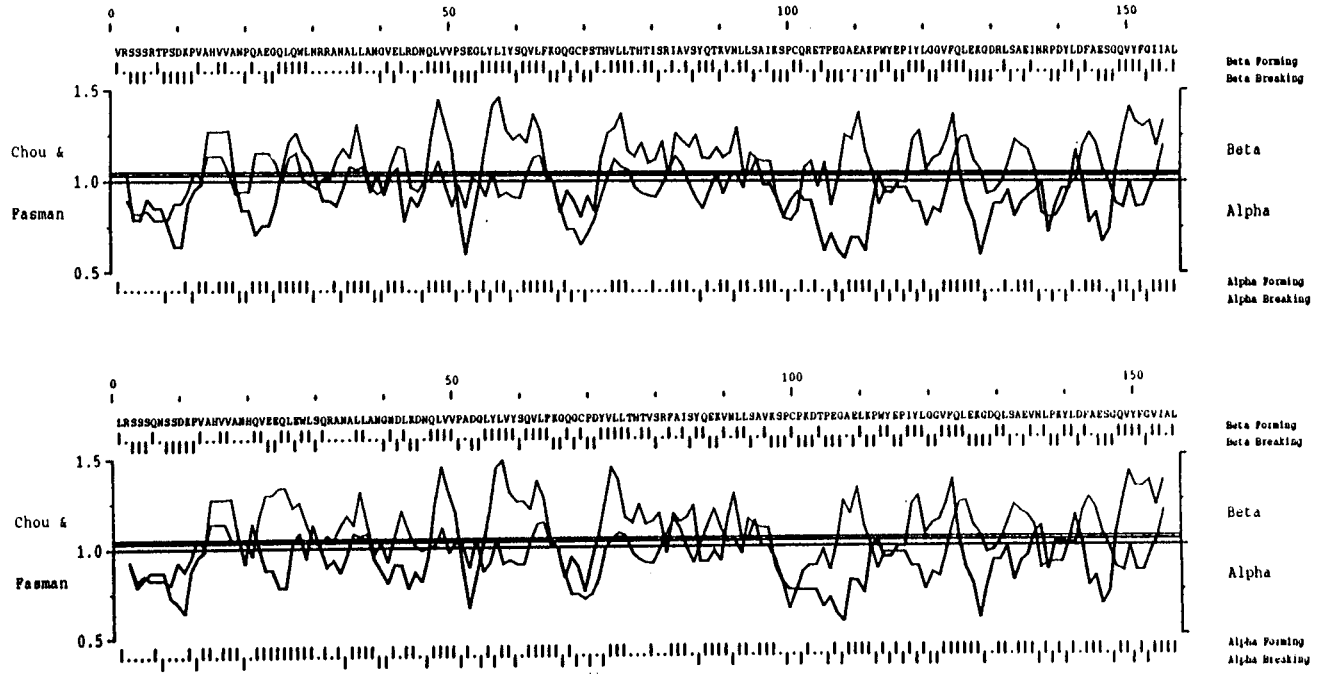

FIGURE 3: Secondary structure prediction based on the amino acid sequence of human TNF-α (upper panel) and murine TNF-α (lower panel) according to the algorithm of Chou and Fasman (1978).

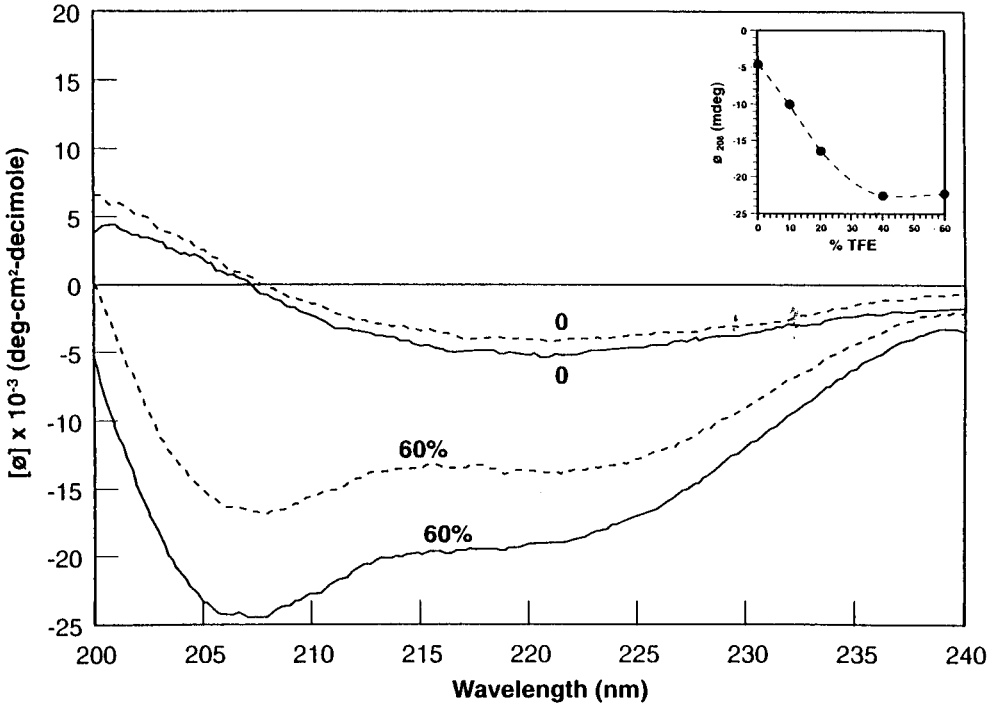

FIGURE 4: Effect of TFE on far-UV CD spectra of human TNF-α (—) and murine TNF-α (- - -). The entire spectrum of both proteins at 0 and 60% TFE is shown, while the inset is a plot of the ellipticity of murine TNF-α at 208 nm versus TFE concentration (percent).

has a propensity for α-helix formation, but long range interactions conferred by the tertiary structure force it to form β-sheet structure. It is difficult to compare the CD spectra of the TFE-unfolded with the thermal-denatured TNF-α due to an increased level of noise in the thermal scans and the fact that good spectra cannot be acquired below 200 nm at elevated temperatures, due to technical limitations. However, there are differences between the spectra in the ratio of ellipticity at 208 and 222 nm, perhaps due to differences in the amount of β-structure and loops retained following denaturation under these different conditions. The TFE-denatured human and murine TNF-α have spectra which more closely resemble classic α-helical peptide spectra, while the thermal-denatured proteins appear to contain more β- or loop structure. Neither the spectra of the thermally denatured TNF-α nor those of the TFE-denatured TNF-α could be accurately deconvoluted.

We have also used sedimentation velocity to investigate the state of association of TFE-denatured TNF-α at a protein concentration of ~60 μg/mL. In 60% TFE, both human and murine TNF-α are clearly not large aggregates and both exhibit sedimentation coefficients of only <0.3 S (in large part due to the very high solvent density of 1.256, which strongly reduces the net sedimentation force). This small sedimentation coefficient probably indicates that they are monomeric, but it is difficult to interpret these data due to

the unknown amount of TFE and water bound to the protein and the profound influence of high levels of TFE on the solvent properties.

As mentioned previously, human TNF-α is very insoluble and aggregated in 10 or 20% TFE. In 20% TFE, murine TNF-α contains a substantial amount of very high-molecular weight aggregates, but the remainder is largely monomeric. In 10% TFE, murine TNF-α consists of trimers plus larger oligomers (with sedimentation coefficients of ∼3−10 S) and little if any monomer. Thus, in summary, it is likely that the increased helicity in murine TNF-α at low TFE concentrations is due to the aggregate component and also that the spectral differences between thermally denatured and 60% TFE-denatured TNF-α may be a consequence of their different states of association. At high TFE concentrations, a transient monomer also appears.

Structural Comparison of Human and Murine TNF-α. In order to understand why human and murine TNF-α behave differently upon unfolding, we have characterized their conformations by CD, fluorescence, and FTIR and their associations by sedimentation equilibrium and SEC. The near- and far-UV CD spectra of both proteins are similar, suggesting that they have similar secondary and tertiary structures. The far-UV CD is consistent with both proteins containing only β-sheet or turn and loop structures but no α-helix. Curve fitting indicates that both proteins contain approximately 50% β-sheet (Chang et al., 1978).

Infrared spectroscopy often gives information about secondary structure complementary to that of CD. The second-derivative amide I′ infrared spectra of human and murine TNF-α are shown in Figure 5. Both spectra lack features indicative of α-helix in PBS at pD 7.0 and 30 °C, since there are minimal IR intensities in the 1650−1660 cm^{-1} region assigned to α-helix. The IR results indicate that the conformation of the two forms of TNF-α are highly similar and contain about 60% β-sheet or turns (strong IR band at 1632 cm^{-1}) and a significant amount of irregular structures (IR band at 1645 cm^{-1}) consistent with the CD results, considering the inaccuracy in estimation of β-sheet content by CD. This is also consistent with the crystal structure (Jones et al., 1989; Eck & Sprang, 1989).

We have used sedimentation equilibrium to assess whether there is a difference between murine and human TNF-α in their self-association into trimers. Earlier studies by this technique did not show evidence for concentration-dependent dissociation of the trimers, but these studies either were done at relatively high protein concentrations (loading concentrations of 125−500 μg/mL) (Arakawa & Yphantis, 1987; Wingfield et al., 1987) or were done at only a single concentration (Pennica et al., 1993). We therefore have carried out more extensive concentration-dependent studies, including data at loading concentrations down to 12.5 μg/mL.

Global analysis of 15 data sets for murine TNF-α as an ideal single species provides an excellent fit, returning a best fit M_r of 51 890 with a 95% confidence interval of 51 680 to 52 100. Since this confidence interval includes the sequence M_r for a trimer (52 064), the data are consistent with no dissociation of the trimers. To try to determine the maximum amount of dissociation compatible with the data, a fit was made to a monomer−dimer−trimer association model, with the monomer molecular weight fixed at its sequence M_r. Since it is known that each subunit in the

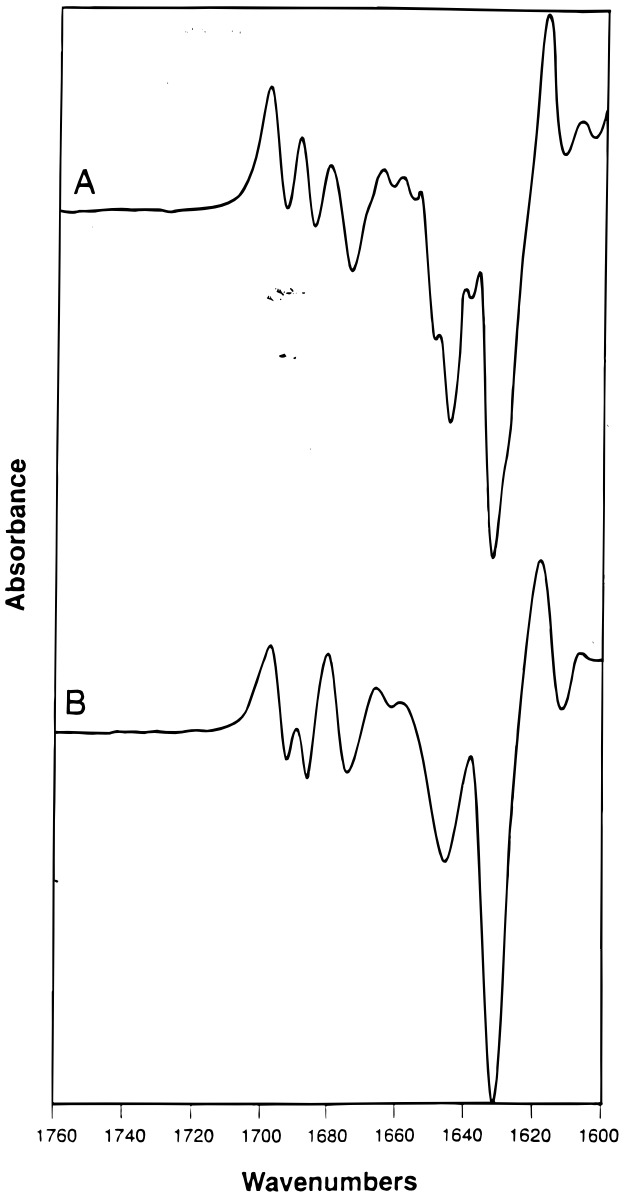

FIGURE 5: Second-derivative amide I′ infrared spectra of (A) human and (B) murine TNF-α in PBS at pD 7.0 and 30 °C.

TNF-α trimer interacts with both its neighbors (Eck & Sprang, 1989), it is reasonable to assume that the binding energy for formation of a dimer will be about $^1/_3$ of that for formation of a trimer, and this assumption was used to simplify the fitting to a single unknown association constant. The resulting best fit for the monomer−trimer association constant is 2.4×10^{17} M^{-2}, implying 50% (wt) dissociation into monomers at a trimer concentration of 130 pM (14 ng/mL total), and that there is a maximum of only 3% monomer at the midpoint of the centrifuge cell even for the lowest-concentration data (4 μg/mL). We therefore regard this value as representing an estimated lower limit for the association constant.

When 18 data sets for human TNF-α are fitted to the single ideal species model, the best fit M_r of 50 210 (50 050 to 50 360) is significantly below the sequence M_r of 52 052 for a trimer. This deviation from the trimer value is outside the maximum ∼2% difference generally found when using a calculated rather than experimental partial specific volume and is therefore probably truly significant. However, the single-species model does provide quite a good fit of the data, and the deviations from the fit do not show the

concentration dependence expected if the lower molecular weight is due to dissociation of trimers. Consistent with this finding, if we fit to the monomer−dimer−trimer association model with the monomer M_r fixed at the sequence value, a poor fit is obtained (90% higher variance, nonrandom residuals).

We do not believe that we are observing dissociation of human TNF-α trimers. Rather, the reason the weight-average M_r is 3.5% below that expected for the trimer is most likely due to the presence of a small fraction (≤5%) of subunits which cannot associate ("incompetent monomer"). We find a larger amount of monomer in samples which have been frozen for a long time. This suggests that the incompetent monomer probably represents a partially unfolded form, whose presence is another consequence of the increased hydrophobicity of human TNF-α. Despite the presence of the incompetent monomer, the lack of concentration dependence of the data again implies a lower limit for the association constant for the competent fraction equivalent to that for the murine protein. Overall, our conclusion from these studies is that we are unable to detect any significant difference in association between the murine and human proteins.

As described above, we have detected no difference in the solution properties of native protein between human and murine TNF-α. However, they showed apparent differences in the elution from SEC−HPLC, which was used to detect dissociation of TNF-α previously (Narhi et al., 1987; Narhi & Arakawa, 1988). The human protein appears to dissociate at protein concentrations of 0.04 mg/mL or lower, with more dissociation occurring at pH 6 than at pH 7. The murine TNF-α, however, elutes as a single symmetric peak corresponding to a trimer under all of these conditions, consistent with the sedimentation equilibrium results. The difference in behavior between human and murine TNF-α upon SEC−HPLC is probably due to the differences in surface hydrophobicity and solubility described above, such that the human TNF-α interacts more strongly with the column matrix and unfolds to a greater extent than the murine protein, resulting in greater apparent dissociation of the protein. SEC analysis using a Superose-12 column also showed nonspecific interactions between human TNF-α, but not murine TNF-α, and the column.

Differences in surface hydrophobicity may be reflected in the binding of ANS, a dye which binds to hydrophobic regions on the surface of proteins, resulting in fluorescence enhancement. The intensity and wavelength of this fluorescence can be used as a qualitative probe of surface hydrophobicity. The human TNF-α binds ANS slightly, with a fluorescence maxima of 4.0 (arbitrary units) at 495 nm in 100 μM ANS. In contrast, the murine TNF-α does not appear to bind ANS at all, such that the spectrum of murine TNF-α in 100 μM ANS is equivalent to that of ANS alone, with a relative maximum of 2 at 515 nm. This indicates that the surface of the folded human molecule is more hydrophobic than that of the folded murine TNF-α. This could account for the differences in solution behavior observed above. The preparation of human TNF-α used was only frozen and thawed one time prior to analysis, and the ANS binding experiment was done under conditions which stabilize the trimer; therefore, the amount of incompetent monomer in the preparation was minimized. However, any incompetent monomer present could contribute to ANS binding.

Scheme 1

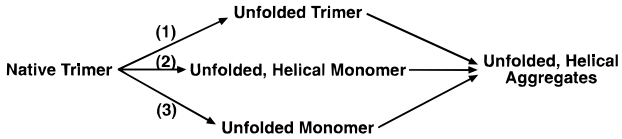

DISCUSSION

Murine TNF-α showed a thermal transition from a primarily β-sheet structure to a structure containing α-helix. The thermal-induced formation of α-helix occurs simultaneously with the loss of tertiary structure and is very insensitive to protein concentration. We have attempted to determine the size of this high temperature-induced helical structure. Dynamic light scattering showed that when murine TNF-α is jumped to 70 °C there is immediate formation of large aggregates, and due to these large aggregates, the possible transient formation of smaller species such as monomers was not observable (data not shown). Sedimentation velocity centrifugation at 25 °C of murine TNF-α following thermal denaturation showed that it also consisted entirely of aggregates. The same sample also contained α-helix by CD. From these results, the heat-denatured state is most likely characterized as unfolded, α-helical aggregates. Three different pathways could lead the native trimer to the unfolded helical aggregate and be consistent with the experimental data, as shown in Scheme 1.

In the first pathway, the native trimer unfolds as a trimer and then associates into helical aggregates. In path 2, the native trimer first unfolds to a helical monomer, which then aggregates, while in pathway 3, the native trimer unfolds to a nonhelical monomer which then associates into a helical aggregate. In all three cases, the thermal transition will be protein concentration-independent as long as the unfolding process, but not the dissociation or aggregation step, is rate-limiting.

In light of the large changes in secondary structures which occur, it is difficult to envision how the trimeric interface could be maintained, as it is in pathway 1. In the other two cases, it is possible that the β-sheet structure present in the native state of the TNF-α may be a consequence of long range interactions conferred by the tertiary structure, or even by trimer formation. The short range interactions in the monomeric state may prefer an α-helical conformation (case 2) or an unfolded conformation (case 3), which can occur only in the state where the long range interactions are eliminated.

The examination of the TNF-α sequence in terms of propensity to form α-helix and β-sheet, according to Chou and Fasman (1978) and shown in Figure 3, indicates that there are many regions in which α-helix-forming amino acids are clustered. This suggests helix formation may be favored in the unfolded monomer (case 2). It has recently been reported that refolding of TNF-α following guanidine hydrochloride denaturation proceeds through several intermediates (Hlodan & Pain, 1995). It is possible that one or more of these intermediates contain α-helix; however, no secondary structure analyses were done in this study, so we cannot determine if the intermediate we have analyzed occurs along this refolding pathway. Alternatively, if α-helix exists only in the aggregate form, then this could be a consequence of long range interactions which occur in the aggregated form but not in the native trimer.

By velocity sedimentation, the TFE-unfolded state appears to consist of aggregates and transient monomers. This would be consistent with TFE-induced unfolding following pathway 2 or 3 but would appear to eliminate pathway 1. The unfolded monomer appears to be very insoluble, being detectable in the presence of high concentrations of TFE only.

The induction of different secondary structures upon unfolding has recently been observed for other proteins. For instance, epidermal growth factor exhibited an α-helical conformation when the disulfide bonds are reduced but only β-sheet structure when the disulfide bonds were formed (Narhi et al., 1992; Prestrelski et al., 1992). Shiraki and colleagues (1995) have also demonstrated the TFE-induced formation of different secondary structures in several proteins, including the formation of α-helix in the β-sheet protein β-lactoglobin. TFE induced significant amounts of α-helix (20−40%) in murine and human TNF-α at neutral pH. This is consistent with the previous observation that an α-helical structure can be induced in human TNF-α by the addition of SDS (Davis et al., 1987). This ability of a protein to assume different secondary structures depending on the presence or absence of long range interactions is very interesting and has implications for protein folding. It is consistent with the results with BPTI (Ittah & Haas, 1995) which implicate both long and short range interactions in the folding pathway of this protein and with the demonstration that the structures adopted by BPTI, myohemerythin, and plastocyanin following unfolding resemble the structure of their peptide fragments or the reduced protein (Dyson et al., 1992a,b; Kimmink & Creighton, 1993; Kwon & Kim, 1994). Thus, TNF-α, if in fact it unfolds through pathway 2 and a similar helical monomer exists as an intermediate in the folding pathway, could be a protein which does not follow the framework model of folding.

In this paper, we have described the thermal- and TFE-induced denaturation of human and murine TNF-α, which results in an α-helical aggregate and demonstrates the importance of both short and long range interactions in the conformation a protein adopts. This reaction is protein concentration-independent and could occur through three different pathways. Additional studies are required to clearly distinguish the three different heat-induced unfolding mechanisms of TNF-α.

REFERENCES

Arakawa, T., & Yphantis, D. A. (1987) *J. Biol. Chem. 262*, 7484−7485.

Briggs, M. S., & Roder, H. (1992) *Proc. Natl. Acad. Sci. U.S.A. 89*, 2017−2021.

Caswell, E. A., Old, L. J., Kassel, R. L., Green, S., Fiere, N., & Williamson, B. (1975) *Proc. Natl. Acad. Sci. U.S.A. 72*, 3666−3670.

Chang, T. C., Wu, C.-S., and Yang, J. T. (1978) *Anal. Biochem. 91*, 13−31.

Chou, P., & Fasman, G. (1978) *Annu. Rev. Biochem. 47*, 251−276.

Clore, G. M., Wingfield, P. T., & Gronenborn, A. M. (1991) *Biochemistry 30*, 2315−2323.

Davis, J. M., Narachi, M. A., Alton, N. K., & Arakawa, T. (1987) *Biochemistry 26*, 1322−1326.

Dyson, H. J., Merutka, G., Waltho, J. P., Lerner, R. A., & Wright, P. E. (1992a) *J. Mol. Biol. 226*, 795−817.

Dyson, H. J., Sayre, J. R., Merutka, G., Shin, H. C., Lerner, R. A., & Wright, P. E. (1992b) *J. Mol. Biol. 226*, 819−835.

Eck, M. J., & Sprang, S. R. (1989) *J. Biol. Chem. 264*, 17599−17605.

Greenfield, M., & Fasman, G. D. (1969) *Biochemistry 8*, 4108−4116.

Hlodan, R., & Pain, R. M. (1995) *Eur. J. Biochem. 231*, 381−387.

Ittah, V., & Haas, E. (1995) *Biochemistry 34*, 4493−4506.

Johnson, M. L., & Faunt, L. M. (1992) *Methods Enzymol. 210*, 1−37.

Johnson, M. L., Correia, J. J., Yphantis, D. A., & Halvorson, H. R. (1981) *Biophys. J. 36*, 575−588.

Jones, E. Y., Stuart, D. I., & Walker, N. C. (1989) *Nature 338*, 225−228.

Kemmink, J., & Creighton, T. E. (1993) *J. Mol. Biol. 234*, 861−878.

Kim, P. S., & Baldwin, R. L. (1990) *Annu. Rev. Biochem. 59*, 631−660.

King, J. (1989) *Chem. Eng. News 67*, 32−54.

Kuwajima, K. (1989) *Proteins: Struct., Funct., Genet. 6*, 87−103.

Kwon, D. W., & Kim, P. S. (1994) *Eur. J. Biochem. 223*, 631−636.

Laue, T. M., Shah, B. D., Ridgeway, T. M., & Pelletier, S. L. (1992) in *Analytical Ultracentrifugation in Biochemistry and Polymer Science* (Harding, S. E., Rowe, A. J., & Horton, J. C., Eds.) pp 90−125, Royal Society of Chemistry, Cambridge.

Lewitt-Bentley, A., Fourme, R., Kahn, R., Prange, T., Vachette, B., Tavernier, J., Hanquier, G., & Niers, W. (1988) *J. Mol. Biol. 199*, 389−392.

Ming, W. J., Bersani, L., & Mantovani, D. (1987) *J. Immunol. 138*, 1469−1474.

Mitraki, A., Fane, B., Haase-Pettingell, C., Sturtevant, J., & King, J. (1991) *Science 253*, 54−58.

Narachi, M. A., Davis, J. M., Hsu, Y.-R., & Arakawa, T. (1987) *J. Biol. Chem. 262*, 13107−13110.

Narhi, L. O., & Arakawa, T. (1987) *Biochem. Biophys. Res. Commun. 147*, 740−746.

Narhi, L. O., Arakawa, T., & Yphantis, D. A. (1987) *J. Biophys. Soc. 53*, 72a.

Narhi, L. O., Arakawa, T., McGinley, M. D., Rohde, M. F., & Westcott, K. R. (1992) *Int. J. Pept. Protein Res. 39*, 182−187.

Narhi, L. O., et al. (1996) *Biochemistry 35*, 11454−11460.

Pan, Y. Q., & Briggs, M. S. (1992) *Biochemistry 31*, 11405−11412.

Pennica, D., Lam, V. T., Weber, R. F., Kohr, W. J., Basa, L. J., Spellman, M. W., Ashkenazi, A., Shire, S. J., & Goeddel, D. V. (1993) *Biochemistry 32*, 3131−3138.

Prestrelski, S. J., Arakawa, T., Kenney, W. C., & Byler, D. M. (1991) *Arch. Biochem. Biophys. 285*, 111−115.

Prestrelski, S. J., Arakawa, T., Wu, C.-S. C., O'Neal, K., Westcott, K. R., & Narhi, L. O. (1992) *J. Biol. Chem. 267*, 319−322.

Ropson, I. J., & Frieden, C. (1992) *Proc. Natl. Acad. Sci. U.S.A. 89*, 7222−7226.

Ropson, I. J., Gordon, J. I., & Frieden, C. (1990) *Biochemistry 29*, 9591−9599.

Sherry, B., & Cerami, A. (1988) *J. Cell Biol. 107*, 1269−1277.

Shiraki, K., Nishikawa, K., & Goto, Y. (1995) *J. Mol. Biol. 245*, 180−194.

Susi, H., & Byler, D. M. (1983) *Biochem. Biophys. Res. Commun. 115*, 391−397.

Varley, P., Gronenborn, A. M., Christenson, H., Wingfield, R. T., Pain, R. H., & Clore, G. M. (1993) *Science 260*, 1110−1111.

Wilkinson, K. D., & Mayer, A. M. (1986) *Arch. Biochem. Biophys. 250*, 390−399.

Wingfield, P., Pain, R. H., & Craig, S. (1987) *FEBS Lett. 211*, 179−184.

Yamada, M., Furutani, Y., Notake, M., Yamagishi, J., Yamayoshi, M., Fukui, T., Nomura, H., Komiya, M., Kuwashima, J., Nakano, K., Sohmura, Y., & Nakamura, S. (1985) *J. Biotechnol. 3*, 141−153.

Yamagishi, J., Kawashima, H., Ohne, M., Matsuo, N., Yamayoshi, M., Fukui, T., Nakata, K., Kotani, H., Furuta, R., Nakano, K., & Yamada, M. (1989) *Int. J. Immunopathol. Pharmacol. 2*, 191−202.

BI952766V